Received: 8 June 2022 | Revised: 19 September 2022 | Accepted: 19 September 2022

DOI: 10.1002/rcm.9404

RESEARCH ARTICLE

Rapid Communications in Mass Spectrometry WILEY

# Removal of contamination in helium for precise $SF_6$-based $\Delta^{36}S$ measurements

Xiaoxiao Yu [1,2] | Binyan Yin [1,3] | Mang Lin [1,2,3]

[1]State Key Laboratory of Isotope Geochemistry and CAS Center for Excellence in Deep Earth Science, Guangzhou Institute of Geochemistry, Chinese Academy of Sciences, Guangzhou, China

[2]Southern Marine Science and Engineering Guangdong Laboratory (Guangzhou), Guangzhou, China

[3]University of Chinese Academy of Sciences, Beijing, China

**Correspondence**
Xiaoxiao Yu and Mang Lin, State Key Laboratory of Isotope Geochemistry and CAS Center for Excellence in Deep Earth Science, Guangzhou Institute of Geochemistry, Chinese Academy of Sciences, Guangzhou, 510640, China.
Email: yuxiaoxiao@gig.ac.cn and linm@gig.ac.cn

**Funding information**
Key Research Program of Frontier Sciences from the Chinese Academy of Sciences, Grant/Award Number: ZDBS-LY-DQC035; the Key Special Project for the Introduced Talents Team of the Southern Marine Science and Engineering Guangdong Laboratory (Guangzhou), Grant/Award Number: GML2019ZD0308; the Guangdong Pearl River Talents Program, Grant/Award Number: 2019QN01L150

**Rationale:** Quantifications of quadruple sulfur isotopic compositions ($\delta^{34}S$, $\Delta^{33}S$, and $\Delta^{36}S$) of sulfur-bearing compounds in nature are valuable for providing new insights into the Earth's evolution such as the crust–mantle cycle, oxygenation of atmosphere and oceans, and the origin and evolution of early life. $SF_6$-based isotope ratio mass spectrometry is the most widely used method of quantification, but $\Delta^{36}S$ measurements at high precision and accuracy have always been technically difficult due to the low abundance of $^{36}S$ (~0.01%). In this paper, we identify a major source of isobaric interferences (i.e., contamination in helium carrier gas in the gas chromatography purification step) and propose a simple strategy to solve this problem.

**Methods:** An $SF_6$ fluorination and purification system was built. Laboratory $SF_6$ reference gas and international $Ag_2S$ standard (IAEA-S1) were used as reference materials to test our method. Contamination from helium carrier gas (99.999%) was purified by a simple two-step cryogenic method to allow for accurate and precise measurements of $\Delta^{36}S$ using the $SF_6$-based isotope ratio mass spectrometry method.

**Results:** Without proper purification of helium carrier gas, large errors in $\Delta^{36}S$ measurements were found. Measured $\Delta^{36}S$ values of $SF_6$ with trace contamination from helium were >10‰ higher than expected values. Using a newly developed purification strategy, the difference in $\Delta^{36}S$ values of $SF_6$ before and after passing through the gas chromatography is less than instrumental errors (<0.2‰). Our improved method yielded an overall $\Delta^{36}S$ precision for IAEA-S1 of 0.12‰ ($n = 6$). This precision is comparable to that found by other laboratories around the world.

**Conclusion:** Our simple two-step cryogenic method significantly improved the accuracy and precision of $\Delta^{36}S$ measurements and is therefore recommended for future determination of quadruple sulfur isotopic compositions in natural samples.

## 1 | INTRODUCTION

Sulfur is the eighth most abundant element in the bulk Earth, occurs in diverse valence states, and has complex redox behaviors in the Earth's interior and surface.[1] Sulfur isotope ratios, which vary subtly in biotic and abiotic transformation processes,[2] are usually measured to better understand the transformation pathways of sulfur between different reservoirs, and to trace the deep and surface sulfur cycle in modern times and the geological past.[3] Sulfur has four stable isotopes, $^{32}S$, $^{33}S$, $^{34}S$, and $^{36}S$, with abundances of approximately 95.04%, 0.75%, 4.20%, and 0.01%, respectively.[4] In the geochemistry community, their ratios are conventionally given in delta notations as:

$$\delta^{3x}S = \left(\frac{^{3x}R_{sample}}{^{3x}R_{reference}} - 1\right) \quad (1)$$

  

where $x$ equals 3, 4, or 6 and $^{3x}R = {}^{3x}S/{}^{32}S$ is the isotopic ratio for samples ($R_{sample}$) or reference materials ($R_{reference}$), usually referred to as the Vienna Cañon Diablo Troilite (VCDT).[5]

In most physical and chemical processes, fractionation of all the sulfur isotopes follows a mass-dependent fractionation (MDF) rule.[3,6,7] Thus, once we measure one sulfur isotope ratio, $\delta^{34}S$ for example, the other two ($\delta^{33}S$ and $\delta^{36}S$) can be calculated following their approximated MDF reference lines.[8] Hulston and Thode[9,10] first proposed that deviations of $\delta^{33}S$ and $\delta^{36}S$ from their MDF lines in iron meteorites might be used to identify nuclear processes such as long-term exposures to high-energy galactic cosmic rays that produces excessive $^{33}S$ and $^{36}S$ atoms via spallation of iron. To quantify the deviations, nonzero capital delta notations for $^{33}S$ and $^{36}S$ are described as:

$$\Delta^{33}S = \delta^{33}S - \left[\left(1+\delta^{34}S\right)^{0.515} - 1\right] \quad (2)$$

$$\Delta^{36}S = \delta^{36}S - \left[\left(1+\delta^{34}S\right)^{1.9} - 1\right] \quad (3)$$

Given that nonzero $\Delta^{33}S$ and $\Delta^{36}S$ values in iron meteorites originate from nuclear processes,[9,10] it was generally accepted that all chemical reactions follow the MDF rule. Using triple oxygen isotopes as an example, Thiemens and Heidenreich[11] first demonstrated that such deviations can occur in a strictly chemical reaction (i.e., ozone formation), which is referred to mass-independent fractionation (MIF). Chemically induced MIF was later experimentally found in sulfur isotope systematics by Bains-Sahota and Thiemens,[12] and subsequently observed in natural samples such as Archean sediments.[13] The large $\Delta^{33}S$ (>0.3‰) and $\Delta^{36}S$ anomalies in Archean sediments are conventionally interpreted as originating from ultraviolet-induced SO-$SO_2$ photochemistry[14] and therefore are considered to be the most solid evidence so far for an extremely low oxygen level in the Archean atmosphere (<$10^{-5}$ present level of atmospheric oxygen).[15,16] After more than 20 years of investigations, sulfur-mass-independent fractionation (S-MIF) has been extensively used to identify and trace the Great Oxidation Event,[17] recycling of Archaean crust,[18] atmosphere chemistry of Mars[19] and modern Earth.[20,21] Recent studies have pointed out that other nonphotochemical reactions such as thermal sulfate reduction[22,23] and elemental sulfur recombination[24–26] may also account for the S-MIF observations in natural samples. The development of high-precision $\Delta^{33}S$ analysis techniques also allows us to resolve low-temperature MDF processes in which isotopes slightly deviate from the MDF reference array.[13,27,28] High-precision measurements of multiple sulfur isotopes focusing on small $\Delta^{33}S$ values (<0.3‰) have been used in understanding marine biogeochemical processes such as Proterozoic microbial activities[29] and anoxic water shoaling in mass extinction events,[30] although interpretations of $\Delta^{36}S$ data remain limited due to the large uncertainties in $\Delta^{36}S$ measurements. These advances were recently reviewed by Thiemens and Lin.[3] In biogeochemical applications and physiochemical investigations, the slope of $\Delta^{36}S/\Delta^{33}S$ is one of the key indicators to delineate the underlying mechanisms and their geochemical implications,[25,31] and therefore accurate and precise determinations for both $\Delta^{33}S$ and $\Delta^{36}S$ are required.

For quadruple sulfur isotope measurements ($\delta^{34}S$, $\Delta^{33}S$, and $\Delta^{36}S$), the conventional $SF_6$-based gas-source isotope-ratio mass spectrometry (IRMS) method[9,10] is the most accurate and precise technique. This method converts sulfur-bearing compounds to $SF_6$ by reactions with $BrF_5$,[12] $F_2$,[27] or $CoF_3$,[32] and purified $SF_6$ is introduced into IRMS as analyst. Because there is only one isotope in fluorine (i.e., $^{19}F$), isobaric interferences from oxygen isotopes in the $SO_2$-based method can be eliminated. Recently, secondary ion mass spectrometer (SIMS) and multiple collector inductively coupled plasma mass spectrometry (MC-ICP-MS) approaches have been developed, but they possess relatively large uncertainties and are only useful for samples with large S-MIF signatures (e.g., $\Delta^{33}S$ > 0.1‰ and $\Delta^{36}S$ > 0.5‰).[33–35] For many studies using the $SF_6$-based IRMS method, $\Delta^{36}S$ values are either not reported or not interpreted, especially in samples with small sulfur amounts.[36,37] The omission of $\Delta^{36}S$ is because of the large $\Delta^{36}S$ analytical errors rooted in part in the low abundance of $^{36}S$. Extremely low abundances of contaminants such as $CO_2$, C-F, S-O-F or hydrocarbon compounds[26,38,39] introduced during the pretreatment processes may lead to significant isobaric interferences in the ionization and measurement steps in IRMS, and therefore hinder precise and accurate measurements of $\Delta^{36}S$ ($^{36}SF_5^+$).[26,38,40] Such contaminants are difficult to completely separate out through cryogenic and gas chromatography (GC) purification,[39] and their origins remain elusive.

In our study, we identified high-purity helium carrier gas used in the GC purification step as one of the major sources of these contaminants. We further developed a two-step cryogenic protocol to purify helium carrier gas. Our new method greatly improved the accuracy and precision of quadruple sulfur isotopic composition measurements, especially for $\Delta^{36}S$.

## 2 | EXPERIMENTAL

### 2.1 | System description

The $SF_6$ fluorination system (Figure 1) was newly built at the State Key Laboratory of Isotope Geochemistry of the Guangzhou Institute of Geochemistry, Chinese Academy of Sciences (GIGCAS). Our $SF_6$ fluorination system mainly follows that of the University of California San Diego originally developed by Bains-Sahota and Thiemens,[12] with some improvements for purification efficiency and laboratory safety. The system consists of three parts: fluorination, extraction, and purification (Figure 1). Specifically, $Ag_2S$ is fluorinated by $BrF_5$ (Dongxiang, China) in nickel reaction tubes to generate $SF_6$. $BrF_5$ stored in KEL-F® (polychlorotrifluoroethylene) traps is used as the fluorination reagent, and is purified through three cryogenic distillation cycles at −196°C and −75°C (ethanol and dry ice) in the system.[41] Waste $BrF_5$ and fluorination byproducts from the experiments, such as HF and $Br_2$, are collected by a stainless-steel

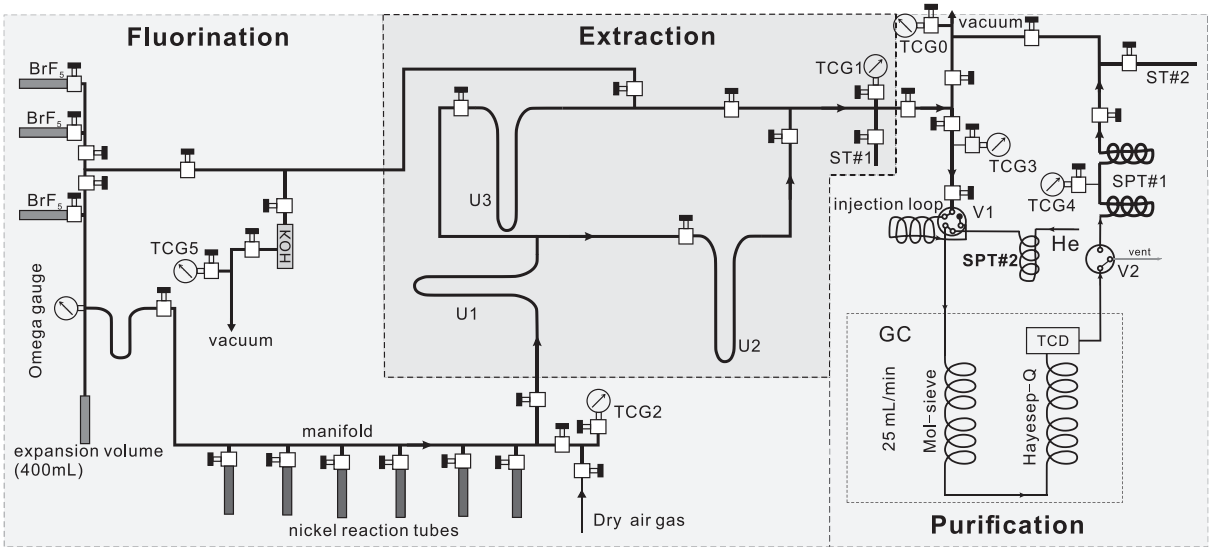


**FIGURE 1** Schematic graph of the vacuum system for $Ag_2S$ fluorination and $SF_6$ purification at GIGCAS. The solid bold and fine lines represent 1/4 and 1/8 in. outer diameter stainless-steel tubes (Swagelok). U1–3, cold traps; TCG0–5, thermocouple gauges; V1–2, multiport values; SPT#1–2, spiral traps; ST#1–2, sample tubes; TCD, thermal conductivity detector; KOH, potassium-hydroxide-filled cold trap (see main text)

trap filled with KOH pellets. Three U-shaped traps are employed in the extraction process for preliminary cryogenic purification. A gas chromatograph (Agilent 8860) is used in the purification process for final purification. Most valves in the systems are stainless-steel bellows sealed valves (Swagelok, SS-4BK).

## 2.2 | Fluorination, extraction, and purification procedures

The fluorination, extraction, and purification procedures mostly follow Lin and Thiemens[26] with some improvements. The reaction and extraction parts were vacuum-pumped by a rotatory pump (Welch, CRVpro6) overnight through U1 and U3 at liquid nitrogen temperature before loading the samples. The dynamic vacuum in the system was better than 0.01 Pa. During vacuum-pumping, the nickel reaction tubes were heated (with cooling circulating water for valve protection) at 250°C to remove any remaining $H_2O$, $BrF_5$, and HF. Before opening the nickel reaction tubes to the air to load the $Ag_2S$ samples, the tubes were filled at room temperature with 1 atmosphere of dry air gas from a gas tank (Kaiyi) to minimize the contamination of $H_2O$ from the air. The nickel reaction tubes containing dry air were then re-closed and subsequently disassembled by unscrewing the vacuum coupling radiation (VCR) connectors between the valves and the tubes. The disassembled nickel reaction tubes were immediately reversed and knocked to remove any possible remaining solid powder from previous fluorinations, and approximately 2.5 mg (~10 μmol) $Ag_2S$ sample preloaded in a silver capsule (3.5 × 9 mm; Santis) was subsequently dropped into the nickel reaction tubes carefully before reconnecting the tubes to the system. The total time for loading each sample was usually <90 s so that contamination of water vapor from air was minimized. The nickel reaction tubes containing the $Ag_2S$ samples were gently (at <0.13 Pa, monitored by TCG1) pumped through U1 and U3 at liquid nitrogen temperature. Once a relatively high vacuum (<0.13 Pa) was achieved, any water possibly absorbed on $Ag_2S$ samples, silver capsules, or inner walls of nickel reaction tubes was removed by heating the nickel reaction tubes for 2 h at 250°C. After a careful vacuum leak check of the nickel reaction tubes through TCG2, 10-times excess stoichiometry required $BrF_5$ measured by an omega gauge was transferred to the tubes and reacted with $Ag_2S$ at 350°C for 15 h or at 550°C for 10 h. As shown in Figure S1, any differences in fluorination temperatures and time in this study did not change our results. During the reaction, the liquid nitrogen surrounding U1 (Figure 1) was removed and U1 was pumped to vacuum through U3 at liquid nitrogen temperature to remove any frozen $BrF_5$.

After reaction, the $SF_6$ produced as well as residual $BrF_5$ were frozen in the nickel tubes at liquid nitrogen temperature for >15 min. Before extraction, the U3 bypass was closed and the clean U2 bypass was opened and pumped to vacuum. Any noncondensable gases such as oxygen (a product of reaction between $BrF_5$ and trace $H_2O$) in the nickel reaction tubes were subsequently pumped away through U1 and U2 at liquid nitrogen temperature. Afterwards, U2 was isolated and the $SF_6$ in the nickel tubes was released at −119°C (ethanol slush) and transferred into U1 at liquid nitrogen temperature (Figure 1). These cryogenic distillation and purification procedures were repeated three more times by transferring $SF_6$ from U1 to U2, from U2 to ST#1, and finally from ST#1 to the GC injection loop (Figure 1). The $SF_6$ in the GC injection loop was released at a room temperature water bath and further carried by high purity helium gas (99.999%; MS Messer Gas Co., Ltd) and injected into the GC by turning the six-way valve V1. The GC was equipped with a 2.7-m

5 Å mol-sieve column (1/8 in. outer diameter [OD]) and a 4.0-m Hayesep-Q column (1/8 in. OD) and operated at an He flow rate of 25 ml/min and 40°C. The $SF_6$ peak was monitored by a thermal conductivity detector in the GC. The purified $SF_6$ was then quantitatively collected into SPT#1 at liquid nitrogen temperature within a 3-min window by switching the three-way valve V2 (Figure 1). Finally, the $SF_6$ in SPT#1 was released at a room temperature water bath and quantitatively transferred into a stainless-steel sample tube (ST#2) at liquid nitrogen temperature for 15 min. After each run, the 2.7-m 5 Å mol-sieve column was back-flushed for 30 min at 200°C to remove any trace contaminants such as $CO_2$ and $SF_6$ that may co-elute in subsequent samples. The 4.0-m Hayesep-Q column was also simultaneous flushed with helium for 30 min at 200°C to the vent port at the three-way valve V2 (Figure 1). After the experiments, the nickel reaction tubes containing $BrF_5$ and other fluorination byproducts were cleaned by heating them to 250°C and pumping for 2 h through U3 (at liquid nitrogen temperature). Eventually, the $BrF_5$ and fluorination byproducts frozen in U3 are transferred into the stainless-steel trap filled with KOH pellets (Figure 1).

Based on the protocol outlined above, the fluorination of two kinds of $Ag_2S$ samples was carried out to identify any problem, especially in $\Delta^{36}S$ measurements. As shown in Section 3, we found that contaminants in the helium carrier gas of GC are responsible for large $\Delta^{36}S$ errors. In our improved protocol, an additional trap (SPT#2) at liquid nitrogen temperature was added to remove impurities in the carrier gas. In addition, we used ethanol slush at −95 ± 5°C instead of a room temperature water bath to release frozen $SF_6$ in SPT#1 to ST#2 (Figure 1). Detailed comparisons of the analytical results are presented and discussed in Section 3.

### 2.3 | Isotope-ratio mass spectrometry

The purified $SF_6$ was finally transferred into the isotope-ratio mass spectrometer and measured in dual inlet mode. Our spectrometer was equipped with a 10 keV acceleration voltage and has four Faraday cups with $1 \times 10^9$, $3 \times 10^{11}$, $1 \times 10^{11}$, and $1 \times 10^{13}$ Ω amplifiers to determine masses of 127, 128, 129, and 131 corresponding to $^{32}SF_5^+$, $^{33}SF_5^+$, $^{34}SF_5^+$, $^{36}SF_5^+$, respectively. The dynamic amplifiers have a range up to 50 V. Every measurement consists of 10 cycles with 12 s of integration time and 15 s of idle time for each cycle. In this study, measured isotopic ratios (Equation 1) are reported versus our laboratory reference $SF_6$ gas ($SF_6$Sub_ST#1).

## 3 | RESULTS AND DISCUSSION

### 3.1 | Large $\Delta^{36}S$ errors due to contamination from helium

In the early stage of our study, we carried out replicated fluorination of our laboratory standard $Ag_2S$ (99.995% metals basis, Macklin; Comm_$Ag_2S$#1) ($n = 6$) and international $Ag_2S$ reference material IAEA-S1 ($n = 5$). Figure 2 shows the multiple sulfur isotopic compositions relative to our laboratory reference gas $SF_6$Sub_ST#1 obtained for Comm_$Ag_2S$#1 and IAEA-S1 during the early stage of this study. The average $\delta^{34}S$ values (±1 standard deviation) for Comm_$Ag_2S$#1 and IAEA-S1 were 16.63 ± 0.34‰ and 3.64 ± 0.22‰ (Figure 2A), respectively. The average values of $\Delta^{33}S$ were −0.038 ± 0.009‰ and 0.067 ± 0.008‰ (Figure 2B), respectively. The average $\Delta^{36}S$ values were −4.27 ± 5.56‰ and 0.31 ± 0.32‰ (Figure 2C), respectively. The precisions of $\Delta^{33}S$ and $\delta^{34}S$ (<0.01‰ and <0.4‰, respectively) are comparable to previous studies,[40] but standard deviations of $\Delta^{36}S$ for both Comm_$Ag_2S$#1 and IAEA-S1 are significantly larger than those reported from other laboratories (≤0.2‰).[27,39,42] In particular, $\Delta^{36}S$ values for the first three fluorination of Comm_$Ag_2S$#1 are extremely large and highly variable

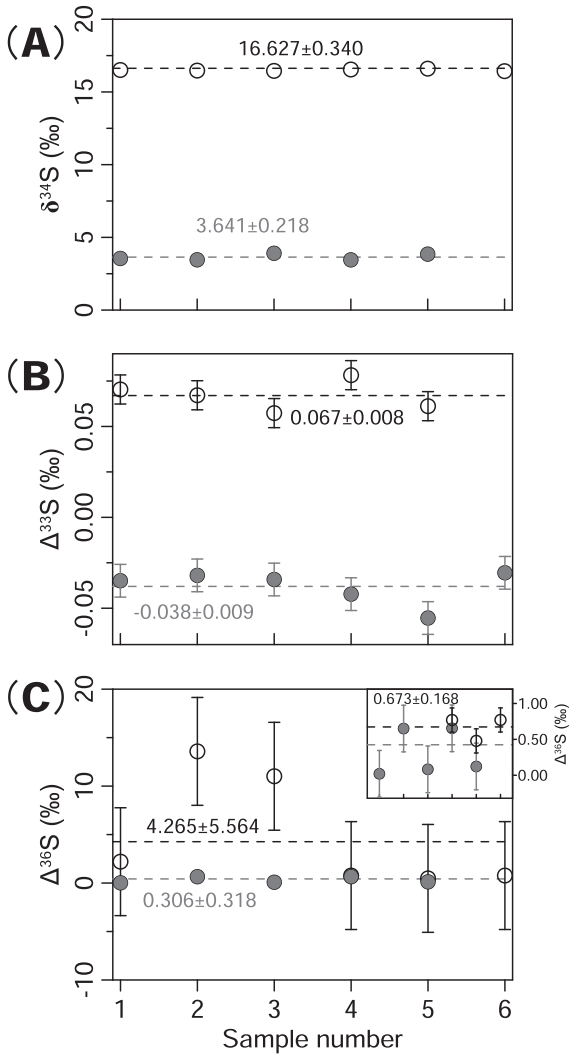


**FIGURE 2** Quadruple sulfur isotope data for Comm_$Ag_2S$#1 (black circles) and IAEA-S1 (gray circles) respective to $SF_6$Sub_ST#1 during our early experiments. Error bars stand for ±1 standard deviations of all measurements, and some error bars are not shown because they are smaller than the symbols

(2.20‰, 13.58‰, and 11.01‰) (Figure 2C), which may be due to unknown impurities in new nickel tubes. The problem was minimized as we kept fluorinating, but the $\Delta^{36}S$ errors of IAEA-S1 remain too high (0.32‰) to accept.

To identify the source of large $\Delta^{36}S$ uncertainties, we transferred $SF_6$Sub_ST#1 from ST#1 into nickel reaction tubes through U1 and U2, and then repeated the fluorination, extraction, and purification procedures outlined in Section 2.2. The $\Delta^{36}S$ values of collected $SF_6$ products were consistently higher (0.43 ± 0.12‰, n = 5) than the expected $SF_6$Sub_ST#1 value (i.e., 0‰). Isotope fractionation is unlikely as such fractionation is not found in both $\Delta^{33}S$ and $\delta^{34}S$. This test therefore suggests that $SF_6$Sub_ST#1 was likely contaminated in our fluorination system, which may be due to vacuum line leakage, elution of GC columns (i.e., adsorption and release),[39] and/or contamination in the carrier helium gas itself. It is well known that trace contamination of carbon-bearing species (e.g., $CO_2$) may lead to anomalously high $\Delta^{36}S$ values because these contaminants may interact with $SF_6$ and ionize to $^{12}C_3F_5^+$ in the IRMS gas source, which has the same mass as $^{36}SF_5^+$ and artificially increases the $^{36}S$ signal.[26] Early work has showed that such compounds may not be completely removed by GC columns.[39,43] We first tested if there was any possible leakage. Replicated static vacuum line leak checks showed that changes in pressure were always <0.13 Pa in 5 min, suggesting that contamination due to leakage is unlikely. We further transferred $SF_6$Sub_ST#1 into the vacuum line and re-collected without passing through the GC. The final deviations of $\Delta^{36}S$ values of $SF_6$Sub_ST#1 from the initial values were within the analytical uncertainties of IRMS (<0.2‰). The test allowed us to exclude vacuum line leakage as a contaminant source, and the GC purification step is therefore likely to be the major error source of $\Delta^{36}S$ measurements.

We next transferred our reference gas $SF_6$Sub_ST#1 from ports ST#1 to ST#2 through the GC following the standard protocol. The average $\Delta^{36}S$ value for re-collecting $SF_6$Sub_ST#1 was 1.18 ± 0.48‰ ($n = 10$) (Table S1), clearly showing contamination of $SF_6$ during the GC purification step. As the GC columns were extensively heated and cleaned before each measurement, we suspected that the large errors for $\Delta^{36}S$ most likely came from the helium carrier gas itself. To test this hypothesis, we first changed the $SF_6$ peak collection time from 3 to 10 min. The 10-min collection time led to a higher $\Delta^{36}S$ value (2.06‰) than the 3-min collection time (1.18 ± 0.48‰, $n = 10$), suggesting that more contaminants were collected along with $SF_6$. We further collected contaminants from the helium directly at high flow (~300–880 ml/min) without passing through the GC columns. The concentrated condensable materials from helium were subsequently released at room temperature and mixed with our reference gas $SF_6$Sub_ST#1. The average $\Delta^{36}S$ value of $SF_6$Sub_ST#1 mixed with contaminants in helium was 12.74 ± 8.16‰ ($n = 7$) (Table S2), strongly suggesting that the impurities are from the carrier gas itself.

With the aim of removing the contaminants in the helium (e.g., trace $H_2O$, $O_2$, $CO_2$, $H_2$, and hydrocarbon), Agilent gas clean traps (2400-B-104 and RMSH-2) were added to the helium tank. However, the problem remained unsolved and te $\Delta^{36}S$ values of our reference gas passing through the GC remained highly variable (up to 75.02‰). We therefore do not recommend using these Agilent gas clean traps for $SF_6$ analysis. Another purification protocol is needed.

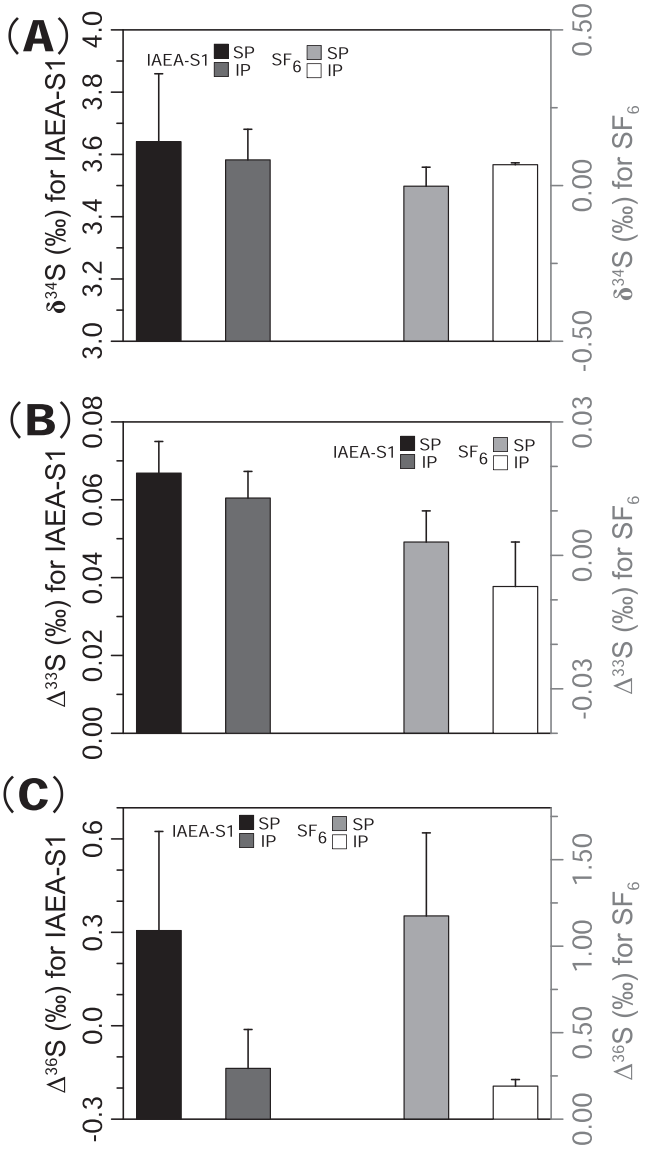


**FIGURE 3** Comparisons of quadruple sulfur isotope measurements of IAEA-S1 and $SF_6$Sub_ST#1 using the standard (SP) and improved (IP) procedures. Significant improvements in both accuracy and precision were found in $\Delta^{36}S$ measurements (the lowest panel). The theoretical values of $\delta^{34}S$, $\Delta^{33}S$, and $\Delta^{36}S$ for $SF_6$Sub_ST#1 are 0‰

## 3.2 | An improved protocol for purifying helium and $SF_6$

Given that carbon-containing compounds are readily condensed at liquid nitrogen temperature, we tried to add a spiral cold trap SPT#2 (at liquid nitrogen temperature) to the helium tank with the aim of freezing any contaminants (Figure 1). The average $\Delta^{36}S$ value for our

reference gas passing through the GC was 0.45 ± 0.29‰ ($n = 3$; Table S3). These values were significantly smaller than our previous tests without the spiral cold trap SPT#2 (1.18 ± 0.48‰, $n = 10$), but remained slightly higher than the expected value (i.e., 0‰). This suggests that there remain trace impurities in the helium gas that are not completely removed. It is also possible that there are trace contaminants leaking from the GC columns, such as Hayesep-Q.[39] To solve this problem, we used a −95 ± 5°C ethanol slush to keep contaminants in the SPT#1 when we released the collected $SF_6$ from SPT#1 to ST#2. In this test, the average $\Delta^{36}S$ value of the re-collected reference gas passing through the GC was 0.19 ± 0.04‰ ($n = 5$) (Table S4), which is identical to the expected value (0‰) within instrumental uncertainties (<0.2‰). This suggests that impurities in the helium can be significantly removed by our final improved protocol. It is worth noting that both the SPT#2 trap (at liquid nitrogen temperature) and −95 ± 5°C ethanol slush extraction at SPT#1 are required as the $\Delta^{36}S$ value of re-collected reference gas $SF_6$Sub_ST#1 passing through GC (with SPT#1 but without SPT#2) is 1.08‰. Overall, the precision and accuracy in the $\delta^{34}S$, $\Delta^{33}S$, and $\Delta^{36}S$ measurements of re-collected reference gas passing through GC using our improved cryogenic protocol were greatly improved (Figure 3).

**TABLE 1** Multiple sulfur isotopic compositions of IAEA-S1 respective to our working $SF_6$ reference gas following the improved procedure

| No. | $\delta^{34}S$(‰) | $\delta^{33}S$(‰) | $\delta^{36}S$(‰) | $\Delta^{33}S$(‰) | $\Delta^{36}S$(‰) |
|---|---|---|---|---|---|
| 1 | 3.592 | 1.900 | 6.501 | 0.052 | −0.335 |
| 2 | 3.497 | 1.858 | 6.620 | 0.059 | −0.035 |
| 3 | 3.570 | 1.901 | 6.807 | 0.064 | 0.013 |
| 4 | 3.482 | 1.850 | 6.437 | 0.058 | −0.189 |
| 5 | 3.757 | 2.005 | 7.052 | 0.072 | −0.098 |
| 6 | 3.597 | 1.909 | 6.668 | 0.058 | −0.177 |
| Average | 3.583 | 1.904 | 6.681 | 0.060 | −0.137 |
| SD | ±0.098 | ±0.055 | ±0.223 | ±0.007 | ±0.124 |

IAEA-S1 was fluorinated, purified, and measured six times.

To further confirm the validity of our improved method, we fluorinated IAEA-S1 and purified the $SF_6$ product using the two-step cryogenic method outlined above. The average $\delta^{34}S$, $\Delta^{33}S$, and $\Delta^{36}S$ values of IAEA-S1 for the new method were 3.58 ± 0.10‰, 0.060 ± 0.007‰, and −0.14 ± 0.12‰ (Table 1), respectively, showing higher precision than achieved by the standard method used in the early stage of this study (Figure 3). The uncertainties of $\delta^{34}S$, $\Delta^{33}S$, and $\Delta^{36}S$ are close to those of most laboratories around the world (Table 2). Although the accuracy for fluorination is not determined in our study, and may be further tested by measuring inter-laboratory-calibrated IAEA-S2 and S-MIF standards,[44] the $SF_6$ test shown in Figure 3 suggests that the accuracy of our new purification protocol is significantly improved. Given the high overall precisions of our IAEA-S1 measurements (including all uncertainties in fluorination, purification, and IRMS measurements), other standards and natural samples can be easily corrected against the results of the primary reference material IAEA-S1 to the international VCDT scale, and a high accuracy is therefore expected.

## 4 | CONCLUSIONS

This study shows that contamination in helium (GC carrier gas) is a major problem that may lead to large errors in $\Delta^{36}S$ measurements. This finding is not trivial as the GC purification procedure is required

**TABLE 2** Errors (1σ) of multiple sulfur isotope measurements of the IAEA-S1 in different laboratories around the world

| References | 1σ ($\delta^{34}S$ ‰) | 1σ ($\Delta^{33}S$ ‰) | 1σ ($\Delta^{36}S$ ‰) | Laboratory[a] |
|---|---|---|---|---|
| Ono et al.[27,45] | 0.275 | 0.003 | 0.093 | GL |
| Ono et al.[27] | 0.111 | 0.009 | 0.178 | UMD |
| Ono et al.[42] | 0.130 | 0.007 | 0.095 | MIT |
| Labidi et al.[46] | 0.040 | 0.004 | 0.110 | UPD |
| Ueno et al.[32] | 0.360 | 0.011 | 0.150 | TIT |
| Masterson[47] | 0.191 | 0.005 | 0.251 | HU |
| Yang et al.[48] | 0.131 | 0.007 | 0.105 | UPD |
| Defouilloy et al.[49] | 0.173 | 0.006 | 0.282 | UPD |
| Lin et al.[25] | 0.018 | 0.008 | 0.066 | USTC |
| Velivetskaya et al.[50] | 0.140 | 0.020 | 0.220 | FEGI |
| Warke et al.[17] | Not reported | 0.015 | 0.177 | STA |
| This study[b] | 0.217 | 0.008 | 0.316 | GIGCAS |
| This study[c] | 0.098 | 0.007 | 0.124 | GIGCAS |

[a]GL, Geophysical Laboratory, Carnegie Institution of Washington, USA; UMD, University of Maryland, USA; MIT, Massachusetts Institute of Technology, USA; UPD, Université Paris Diderot, France; TIT, Tokyo Institute of Technology, Japan; HU, Harvard University, USA; USTC, University of Science and Technology of China, China. FEGI, Far East Geological Institute, Russia; STA, University of St Andrews, USA.

[b]Standard protocol in this study.

[c]Improved protocol in this study.

in all $SF_6$-based IRMS methods. Given that the global helium supply is mainly from United States, Qatar, Algeria, and Russia, many countries rely on imported helium from foreign countries and industries, and therefore the quality of imported helium depends on suppliers and may be highly variable. Our results reinforce that care is required if positive $\Delta^{36}S$ anomalies are found in natural sample measurements as such anomalies may be an analytical artifact due to impurities in helium. We developed a simple two-step cryogenic method to avoid this problem for high-precision measurements of $\Delta^{36}S$. The standard deviation values of IAEA-S1 in $\delta^{34}S$, $\Delta^{33}S$, and $\Delta^{36}S$ yield following the improved method are 0.10‰, 0.007‰, and 0.12‰, respectively, which are comparable with those obtained from other laboratories. We conclude that our protocol is reliable for determination of quadruple sulfur isotopic compositions in natural samples.

## ACKNOWLEDGMENTS

We thank Prof. Yongbo Peng from the International Center for Isotope Effects Research at Nanjing University for providing the nickel and KEL-F tubes used in this study. Technical discussions with Prof. Mark Thiemens and Teresa Jackson from the University of California San Diego are greatly acknowledged. This work was supported by the Key Research Program of Frontier Sciences from the Chinese Academy of Sciences (ZDBS-LY-DQC035), the Key Special Project for the Introduced Talents Team of the Southern Marine Science and Engineering Guangdong Laboratory (Guangzhou) (GML2019ZD0308), and the Guangdong Pearl River Talents Program (2019QN01L150) to M.L. This is contribution no. IS3249 from GIGCAS.

## CONTRIBUTIONS

M.L. conceived the study. X.Y. and M.L. designed the study. X.Y. and B.Y. performed the study. X.Y. and M.L. analyzed data. X.Y. and M.L. wrote the manuscript.

## PEER REVIEW

The peer review history for this article is available at https://publons.com/publon/10.1002/rcm.9404.

## DATA AVAILABILITY STATEMENT

Data available on request from the authors.

## ORCID

*Xiaoxiao Yu* https://orcid.org/0000-0002-4292-950X

## REFERENCES

1. Dreibus G, Palme H. Cosmochemical constraints on the sulfur content in the Earth's core. *Geochim Cosmochim Acta*. 1996;60(7):1125-1130. doi:10.1016/0016-7037(96)00028-2
2. Shen Y, Buick R. The antiquity of microbial sulfate reduction. *Earth Sci Rev*. 2004;64(3-4):243-272. doi:10.1016/S0012-8252(03)00054-0
3. Thiemens MH, Lin M. Use of isotope effects to understand the present and past of the atmosphere and climate and track the origin of life. *Angew Chem Int Ed Engl*. 2019;58(21):6826-6844. doi:10.1002/anie.201812322
4. Ding T, Valkiers S, Kipphardt H, et al. Calibrated sulfur isotope abundance ratios of three IAEA sulfur isotope reference materials and V-CDT with a reassessment of the atomic weight of sulfur. *Geochim Cosmochim Acta*. 2001;65(15):2433-2437. doi:10.1016/S0016-7037(01)00611-1
5. Robinson BW. Sulphur isotope standards. In: *Reference and Intercomparison Materials for Stable Isotopes of Light Elements, vol. IAEA-TECHDOC-825*. IAEA; 1993:39-45.
6. Thiemens MH. History and applications of mass-independent isotope effects. *Annu Rev Earth Planet Sci*. 2006;34(1):217-262. doi:10.1146/annurev.earth.34.031405.125026
7. Thiemens MH, Lin M. Discoveries of mass independent isotope effects in the solar system: Past, present and future. *Rev Mineral Geochem*. 2021;86(1):35-95. doi:10.2138/rmg.2021.86.02
8. Bigeleisen J, Mayer MG. Calculation of equilibrium constants for isotopic exchange reactions. *J Chem Phys*. 1947;15(5):261-267. doi:10.1063/1.1746492
9. Hulston JR, Thode HG. Variations in the $S^{33}$, $S^{34}$, and $S^{36}$ contents of meteorites and their relation to chemical and nuclear effects. *J Geophys Res*. 1965;70(14):3475-3484. doi:10.1029/JZ070i014p03475
10. Hulston JR, Thode HG. Cosmic-ray-produced $S^{36}$ and $S^{33}$ in the metallic phase of iron meteorites. *J Geophys Res*. 1965;70(18):4435-4442. doi:10.1029/JZ070i018p04435
11. Thiemens MH, Heidenreich JE. The mass-independent fractionation of oxygen: A novel isotope effect and its possible cosmochemical implications. *Science*. 1983;219(4588):1073-1075. doi:10.1126/science.219.4588.1073
12. Bains-Sahota SK, Thiemens MH. Fluorination of sulfur tetrafluoride, pentafluorosulfur chloride and disulfur decafluoride to sulfur hexafluoride for mass spectrometric isotope ratio analysis. *Anal Chem*. 1988;60(10):1084-1086. doi:10.1021/ac00161a029
13. Farquhar J, Bao H, Thiemens M. Atmospheric influence of Earth's earliest sulfur cycle. *Science*. 2000;289(5480):756-758. doi:10.1126/science.289.5480.756
14. Farquhar J, Savarino J, Airieau S, Thiemens MH. Observation of wavelength-sensitive mass-independent sulfur isotope effects during $SO_2$ photolysis: Implications for the early atmosphere. *J Geophys Res: Planets*. 2001;106(E12):32829-32839. doi:10.1029/2000JE001437
15. Pavlov AA, Kasting JF. Mass-independent fractionation of sulfur isotopes in Archean sediments: Strong evidence for an anoxic Archeanatmosphere. *Astrobiology*. 2002;2(1):27-41. doi:10.1089/153110702753621321
16. Lyons TW, Reinhard CT, Planavsky NJ. The rise of oxygen in Earth's early ocean and atmosphere. *Nature*. 2014;506(7488):307-315. doi:10.1038/nature13068
17. Warke MR, Di Rocco T, Zerkle AL, et al. The great oxidation event preceded a Paleoproterozoic "snowball earth". *Proc Natl Acad Sci USA*. 2020;117(24):13314-13320. doi:10.1073/pnas.2003090117
18. Farquhar J, Wing BA, McKeegan KD, Harris JW, Cartigny P, Thiemens MH. Mass-independent sulfur of inclusions in diamond and sulfur recycling on early earth. *Science*. 2002;298(5602):2369-2372. doi:10.1126/science.1078617
19. Franz HB, Kim ST, Farquhar J, et al. Isotopic links between atmospheric chemistry and the deep Sulphur cycle on Mars. *Nature*. 2014;508(7496):364-368. doi:10.1038/nature13175
20. Romero AB, Thiemens MH. Mass-independent sulfur isotopic compositions in present-day sulfate aerosols. *J Geophys Res: Atmospheres*. 2003;108(D16):4524. doi:10.1029/2003JD003660
21. Savarino J, Romero A, Cole-Dai J, Bekki S, Thiemens MH. UV induced mass-independent sulfur isotope fractionation in stratospheric volcanic sulfate. *Geophys Res Lett*. 2003;30(21):2131. doi:10.1029/2003GL018134

22. Watanabe Y, Farquhar J, Ohmoto H. Anomalous fractionations of sulfur isotopes during thermochemical sulfate reduction. *Science*. 2009;324(5925):370-373. doi:10.1126/science.1169289
23. Oduro H, Harms B, Sintim HO, Kaufman AJ, Cody G, Farquhar J. Evidence of magnetic isotope effects during thermochemical sulfate reduction. *Proc Nati Acad Sci USA*. 2011;108(43):17635-17638. doi:10.1073/pnas.1108112108
24. Babikov D. Recombination reactions as a possible mechanism of mass-independent fractionation of sulfur isotopes in the Archean atmosphere of earth. *Proc Natl Acad Sci USA*. 2017;114(12):3062-3067. doi:10.1073/pnas.1620977114
25. Lin M, Zhang X, Li M, et al. Five-S-isotope evidence of two distinct mass-independent sulfur isotope effects and implications for the modern and Archean atmospheres. *Proc Natl Acad Sci USA*. 2018;115(34):8541-8546. doi:10.1073/pnas.1803420115
26. Lin M, Thiemens MH. A simple elemental sulfur reduction method for isotopic analysis and pilot experimental tests of symmetry-dependent sulfur isotope effects in planetary processes. *Geochem Geophys Geosyst*. 2020;21(7):e2020GC009051. doi:10.1029/2020GC009051
27. Ono S, Wing B, Johnston D, Farquhar J, Rumble D. Mass-dependent fractionation of quadruple stable sulfur isotope system as a new tracer of sulfur biogeochemical cycles. *Geochim Cosmochim Acta*. 2006;70(9):2238-2252. doi:10.1016/j.gca.2006.01.022
28. Farquhar J, Johnston DT, Wing BA, et al. Multiple Sulphur isotopic interpretations of biosynthetic pathways: Implications for biological signatures in the sulphur isotope record. *Geobiology*. 2003;1(1):27-36. doi:10.1046/j.1472-4669.2003.00007.x
29. Johnston DT, Wing BA, Farquhar J, et al. Active microbial sulfur disproportionation in the Mesoproterozoic. *Science*. 2005;310(5753):1477-1479. doi:10.1126/science.1117824
30. Shen Y, Farquhar J, Zhang H, Masterson A, Zhang T, Wing BA. Multiple S-isotopic evidence for episodic shoaling of anoxic water during late Permian mass extinction. *Nat Commun*. 2011;2(1):210. doi:10.1038/ncomms1217
31. Ono S. Photochemistry of sulfur dioxide and the origin of mass-independent isotope fractionation in Earth's atmosphere. *Annu Rev Earth Planet Sci*. 2017;45(1):301-329. doi:10.1146/annurev-earth-060115-012324
32. Ueno Y, Aoyama S, Endo Y, Matsu'ura F, Foriel J. Rapid quadruple sulfur isotope analysis at the sub-micromole level by a flash heating with $CoF_3$. *Chem Geol*. 2015;419:29-35. doi:10.1016/j.chemgeo.2015.10.032
33. LaFlamme C, Martin L, Jeon H, et al. In situ multiple sulfur isotope analysis by SIMS of pyrite, chalcopyrite, pyrrhotite, and pentlandite to refine magmatic ore genetic models. *Chem Geol*. 2016;444:1-15. doi:10.1016/j.chemgeo.2016.09.032
34. Paris G, Sessions AL, Subhas AV, Adkins JF. MC-ICP-MS measurement of $\delta^{34}S$ and $\Delta^{33}S$ in small amounts of dissolved sulfate. *Chem Geol*. 2013;345:50-61. doi:10.1016/j.chemgeo.2013.02.022
35. Kümmel S, Horst A, Gelman F, Strauss H, Richnow HH, Gehre M. Simultaneous compound-specific analysis of $\delta^{33}S$ and $\delta^{34}S$ in organic compounds by GC-MC-ICPMS using medium- and low-mass-resolution modes. *Anal Chem*. 2020;92(21):14685-14692. doi:10.1021/acs.analchem.0c03253
36. Peng Y, Bao H, Jiang G, et al. A transient peak in marine sulfate after the 635-ma snowball earth. *Proc Natl Acad Sci USA*. 2022;119(19):e2117341119. doi:10.1073/pnas.2117341119
37. Gong S, Peng Y, Bao H, et al. Triple sulfur isotope relationships during sulfate-driven anaerobic oxidation of methane. *Earth Planet Sci Lett*. 2018;504:13-20. doi:10.1016/j.epsl.2018.09.036
38. Rumble D, Hoering TC, Palin JM. Preparation of $SF_6$ for sulfur isotope analysis by laser heating sulfide minerals in the presence of $F_2$ gas. *Geochim Cosmochim Acta*. 1993;57(18):4499-4512. doi:10.1016/0016-7037(93)90499-M
39. Ono S, Wing B, Rumble D, Farquhar J. High precision analysis of all four stable isotopes of sulfur ($^{32}S$, $^{33}S$, $^{34}S$ and $^{36}S$) at nanomole levels using a laser fluorination isotope-ratio-monitoring gas chromatography–mass spectrometry. *Chem Geol*. 2006;225(1-2):30-39. doi:10.1016/j.chemgeo.2005.08.005
40. Au Yang D, Landais G, Assayag N, Widory D, Cartigny P. Improved analysis of micro- and nanomole-scale sulfur multi-isotope compositions by gas source isotope ratio mass spectrometry. *Rapid Commun Mass Spectrom*. 2016;30(7):897-907. doi:10.1002/rcm.7513
41. Ignatiev AV, Velivetskaya TA, Budnitskiy SY, Yakovenko VV, Vysotskiy SV, Levitskii VI. Precision analysis of multisulfur isotopes in sulfides by femtosecond laser ablation GC-IRMS at high spatial resolution. *Chem Geol*. 2018;493:316-326. doi:10.1016/j.chemgeo.2018.06.006
42. Ono S, Keller NS, Rouxel O, Alt JC. Sulfur-33 constraints on the origin of secondary pyrite in altered oceanic basement. *Geochim Cosmochim Acta*. 2012;87:323-340. doi:10.1016/j.gca.2012.04.016
43. Gao X, Thiemens MH. Systematic study of sulfur isotopic composition in iron meteorites and the occurrence of excess $^{33}S$ and $^{36}S$. *Geochim Cosmochim Acta*. 1991;55(9):2671-2679. doi:10.1016/0016-7037(91)90381-E
44. Geng L, Savarino J, Caillon N, et al. Intercomparison measurements of two $^{33}S$-enriched sulfur isotope standards. *J Anal Atom Spectrom*. 2019;34(6):1263-1271. doi:10.1039/C8JA00451J
45. Ono S, Shanks WC, Rouxel OJ, Rumble D. S-33 constraints on the seawater sulfate contribution in modern seafloor hydrothermal vent sulfides. *Geochim Cosmochim Acta*. 2007;71(5):1170-1182. doi:10.1016/j.gca.2006.11.017
46. Labidi J, Cartigny P, Birck JL, Assayag N, Bourrand JJ. Determination of multiple sulfur isotopes in glasses: A reappraisal of the MORB $\delta^{34}S$. *Chem Geol*. 2012;334:189-198. doi:10.1016/j.chemgeo.2012.10.028
47. Masterson AL. Multiple sulfur isotope applications in diagenetic models and geochemical proxy records. Diss 2016.
48. Yang DA, Landais G, Assayag N, Widory D, Cartigny P. Improved analysis of micro- and nanomole-scale sulfur multi-isotope compositions by gas source isotope ratio mass spectrometry. *Rapid Commun Mass Spectrom*. 2016;30(7):897-907. doi:10.1002/rcm.7513
49. Defouilloy C, Cartigny P, Assayag N, Moynier F, Barrat JA. High-precision sulfur isotope composition of enstatite meteorites and implications of the formation and evolution of their parent bodies. *Geochim Cosmochim Acta*. 2016;172:393-409. doi:10.1016/j.gca.2015.10.009
50. Velivetskaya TA, Ignatiev AV, Yakovenko VV, Vysotskiy SV. An improved femtosecond laser-ablation fluorination method for measurements of sulfur isotopic anomalies ($\Delta^{33}S$ and $\Delta^{36}S$) in sulfides with high precision. *Rapid Commun Mass Spectrom*. 2019;33(22):1722-1729. doi:10.1002/rcm.8528


## SUPPORTING INFORMATION

Additional supporting information can be found online in the Supporting Information section at the end of this article.

**How to cite this article:** Yu X, Yin B, Lin M. Removal of contamination in helium for precise $SF_6$-based $\Delta^{36}S$ measurements. *Rapid Commun Mass Spectrom*. 2022;36(24):e9404. doi:10.1002/rcm.9404